Analysis of Floating Oscillating Water Column (FOWC)-breakwater Hybrid System: A Numerical Study

Giri Ram*[1], Mohd Rashdan Saad*[1], Noh Zainal Abidin*[2] and Mohd Rosdzimin Abdul Rahman*[1]

*[1] Department of Mechanical Engineering, Faculty of Engineering,
Universiti Pertahanan Nasional Malaysia,
Kem Sg. Besi, 57000, Kuala Lumpur, Malaysia

*[2] Department of Science and Maritime Technology,
Faculty of Defence Science and Technology,
Universiti Pertahanan Nasional Malaysia,
Kem Sg. Besi, 57000, Kuala Lumpur, Malaysia

Abstract

This study numerically investigates the performance of a Floating Oscillating Water Column (FOWC)-breakwater Hybrid System using the Computational Fluid Dynamics (CFD) solver Ansys 2021 R1: Fluent. The domain is a two-dimensional numerical wave tank (NWT) with a partially immersed FOWC. Volume of Fluid, finite volume method and RANS equations were used to model and simulate the FOWC-breakwater hybrid system. The meshing process was done by separating the NWT to three segments, with the water surface and the middle segment having a fine element size of 0.005m, which is two times finer than the outer segments. A numerical beach was added 2m from the outlet to minimize the effects of wave reflection to the devices. Firstly, the design of FOWC and numerical setup was validated. Two models, with different top opening sizes and initial conditions were used for validation. Measurements of wave elevation and horizontal velocity were recorded and compared with experimental data from a previous study. Secondly, the FOWC-breakwater hybrid system was modelled and calculated. Four gap ratios and five wave periods were used for comparison. Measurements of wave elevation at various locations of the NWT and inside the FOWC chamber were recorded. Performance coefficients, such as the reflection coefficient, wave elevation ratio and velocity ratio, were derived from the measurements.

1. Introduction

1.1 Background

In response to the threat of climate change, countries are looking into adopting renewable forms energy generation with a low carbon footprint. Recently on 31st October 2021, the United Nations Climate Change Conference (COP26) was held in Glasgow. It concluded with all countries agreeing the Glasgow Climate Pact to keep 1.5°C alive and finalize the outstanding elements of the Paris Agreement. One way to reduce the effects of global warming is to transition from the use of fossil fuel to alternative sources such as wind and ocean wave energy. Ocean wave energy is pollution free and does not contribute to contamination in the environment, besides reducing carbon dioxide emissions (Kharati-Koopaee and Fathi Kelestani, 2020).

1.2 Floating Oscillating Water Column (FOWC)

Ocean wave energy is extracted and converted to electrical energy using a wave energy converter (WEC). There are various types of WECs being researched in current times, the popular ones being Oscillating Water Column (OWC), point absorber and attenuator. The OWC typically consists of a partially submerged chamber with a power take off (PTO) unit at the roof of the chamber. Incident wave causes motion of water surface inside the chamber which then causes expansion and compression of the air column and this generates wave energy.

There are some notable OWCs installed around the world for commercial use, namely a 300kW OWC plant in Mutriku, Spain and 500kW OWC plant in Limpet, Scotland (Samak et al., 2021). While a fixed OWC has been proven to be a commercial success, there are some drawbacks. Because it is installed on coastal structures onshore, the marine ecosystem may be potentially harmed. Besides that, the wave energy load is lower compared to offshore because of the beaching effect that happens onshore. This encouraged research on Floating Oscillating Water Column (FOWC), which as per its name, is a water column that is not mounted on the coastal structure.

1.3 Floating Breakwater

A breakwater functions as a protective barrier that shields the shoreline from the incoming waves of the ocean, thereby sheltering the coastal infrastructure. Mikami et al. (2015) showed that detached floating breakwaters are capable of mitigating the effects of tsunami. Breakwaters also help in mitigating wave storms. An added benefit of the breakwater is that it could also be used to assist in energy conversion, as well as to improve the longevity of WEC. The earlier designs of WEC-breakwater hybrid systems had a bottom-mounted breakwater (Zhao et al., 2019). It was later found that bottom-mounted breakwater is uneconomical in offshore regions, where floating breakwaters become more favorable. (Zhao et al., 2019).

Floating breakwaters are devices that are not mounted on coastal structures and typically float on the surface of the sea. Some of its advantages compared to fixed breakwaters are the low cost of construction, flexibility of design and installation and eco-friendliness (Zhao et al., 2019). Zhang et al. (2021) studied the effects of narrow gap wave resonance and found that gap wave resonance considerably improved the performance of wave extraction. Koutrouvelli (2021) used a composite modelling approach to prove the concept of novel hybrid-WEC system. It was found that the hybrid system is an adequate approach, there is an improvement in the hydraulic performance of breakwater and the negative impact in the structural stability of the overall system in relation integration is negligible.

1.4 FOWC-Breakwater Hybrid System

A well-documented problem in the generation of wave energy is the construction cost of WECs, rendering the price of generated electricity to become uneconomical (Zhao et al., 2019). Therefore, the integration of FOWC-breakwater tackles this problem by being cost-sharing, that reduces the cost of construction, space-sharing by allowing the installation of various devices in small spaces and lastly the multifunctionality of devices, especially that of the breakwater, which functions both to improve wave energy extraction and to shelter nearby devices from the effects of incoming waves (Zhao et al., 2019).

The floating nature of the system also renders additional benefits, such as the ability to be installed offshore. This makes the devices become less threatening to the marine ecosystem living near the shore as well as having a wider area for installation, which avoids competition with other marine activities such as fishing and shipping. The portability of

the floating system also helps in relocating devices to a different site if and when necessary. While there are many benefits to offshore wave energy extraction, a major disadvantage, as highlighted by Chen et al. (2013), is the strong wave impulsive load offshore which may incur a higher maintenance cost compared to onshore. The ability of breakwater to provide protection to the FOWC at regions of high wave impulsive load needs further study.

1.5 Numerical Study

Due to the costly nature of open ocean trials, a high number of studies rely on numerical studies and experimentation in controlled environments (Windt et al., 2021). Of the two, numerical studies are more cost-effective and time-saving. However, depending on the method of calculation used, the accuracy of numerical data to on-site data may vary greatly. A validation to experimental data helps in improving the accuracy of numerical data.

Computational Fluid Dynamic (CFD) method that uses Navier-Stokes equations are widely used for the analysis and development of a WEC and seen to be the best approach by many authors (De Backer, 2009) (Iturrioz et al., 2015). The in-depth analysis of the dynamics of the structure, the discretization of domain into high-resolution meshes and the study of complex behaviors like turbulence are some of the benefits of the CFD method (Iturrioz et al, 2015).

1.6 Performance of FOWC-Breakwater

The performance of WEC was measured in some studies either using capture width ratio or the cost of producing 1 kilowatt-hour (Aderinto and Li, 2019). Some challenges in measuring performance of WECs are firstly, the difficulty to compare different capture technologies, secondly, difference in scales and sized that influence results and thirdly, the effect of wave condition at experimental and installation site (Aderinto and Li, 2019). For He and Huang (2016), energy dissipation of the system was used to measure the performance of the wave absorbers on how much of wave reflection is reduced. Besides that, energy loss due to vortex shedding was calculated. A dimensional analysis was conducted to find reflection coefficient, amplification coefficient, pressure coefficient and energy-extraction efficiency. In Zhang et al. (2021), the performance of the dual-floater WEC-breakwater hybrid system was measured using the values of optimal damping coefficient. Other performance coefficients such as the reflection coefficient, transmission coefficient and dissipation coefficient were also analyzed.

The method used to measure reflection coefficient is the two-point method, which is a method to measure the surface displacement at two points in a time-series model. It was used for Goda and Suzuki (1977) and is still applied in recent studies, such as He and Huang (2016) and Zhang et al. (2020). For Isaacson (1991), it was referred to as Method I: two fixed probes, where two heights and one phase angle is measured. When compared to other methods that use three fixed probes, it was found to have a reasonable accuracy.

1.7 Purpose of Study

The potential for wave energy generation in the offshore region is an interesting prospect for many coastal regions of the world. In addition to that, the breakwater aids in wave energy generation. These advantages prompted the authors of this study to look into the performance of the FOWC-breakwater hybrid system. The first objective was to understand the characteristics and second to study the performance of the FOWC-breakwater hybrid system.

2. Numerical Set-up

2.1 General Set-up

The CFD solver used is ANSYS 2021 R1: Fluent. The models used for study are categorized as in Table 1. Models 1 and 2 are studied for validation purposes, models 3 to 6 are for the study of four different ratios of gap of breakwater relative to FOWC.

Table 1: Models used for study and differences in setting

Model No.	Period (s)	Gap Ratio
1	1.7	None
2	1.3	None
3	1.3-2.2	2
4	1.3-2.2	2.5
5	1.3-2.2	3
6	1.3-2.2	3.5

Volume of Fluid (VOF) method and implicit setting was used. Two phases, namely air and water-liquid phase are selected as in Table 2.

Table 2: Properties of the phases

Material Name	Density (kg/m^3)	Viscosity(kg/ms)
Air	1	1.48e- 3
Water-Liquid	1000	0.1

Wave theory is selected in accordance with the graph for limits of validity for wave theories (LeMéhauté, 1969). Table 3 shows the boundary conditions of numerical model.

Table 3: Setting of boundary condition

Description	Value
Free surface level (m)	0
Bottom level (m)	-0.6
Wave boundary condition option	Shallow/Intermediate Waves
Wave theory	Second Order Stokes
Wave height (m)	0.08
Wave length (m)	2.418-4.893
Wave period (s)	1.3-2.2

Standard initialization with flat-wave open-channel initialization method was used. Other settings to run simulation are shown in Table 4.

Table 4: Settings used to run simulation

Description	Value
Time stepping method	Fixed
Time step size (s)	0.001
Number of time steps	60000
Maximum iterations/Time step	25

2.2 Numerical Set-up for Validation Models

The design for models 1 and 2 are displayed as in Fig. 1. Two-dimensional design of FOWC is displayed in Fig. 2. The FOWC was set to be a homogeneous rigid body that is partially immersed in water-liquid. The model operates in a fixed floating mechanism without translation or rotation; the purpose is to narrow down on the list of variables that affect the results and also to save on computational time. Experimental results from Iturrioz et al. (2015) was used as validation;

the only difference being the removal of the left and right legs, which are seen to have minimal effect on the result. A FOWC draft of 0.2m and a water depth of 0.6m was set with the orifice diameter designed to be 0.05m.
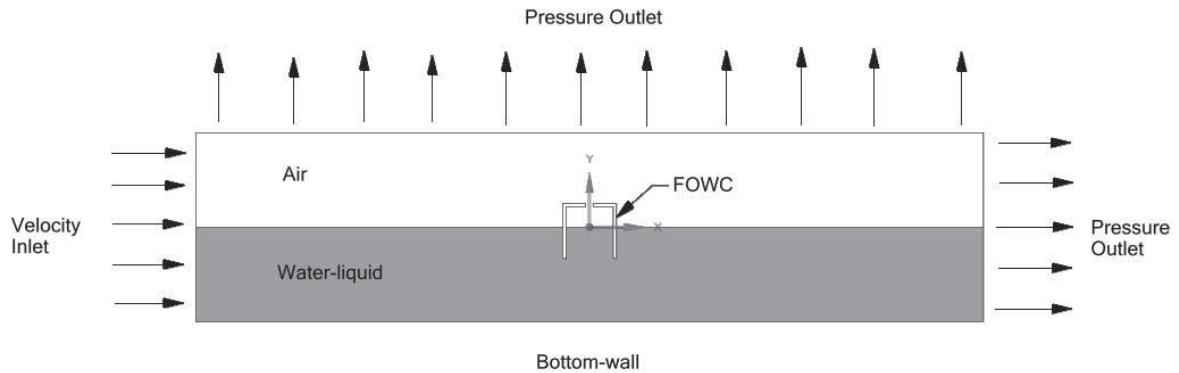

Fig. 1: Schematic of a section of NWT design for models 1 and 2 with material characteristic, dimensions of FOWC and boundary condition
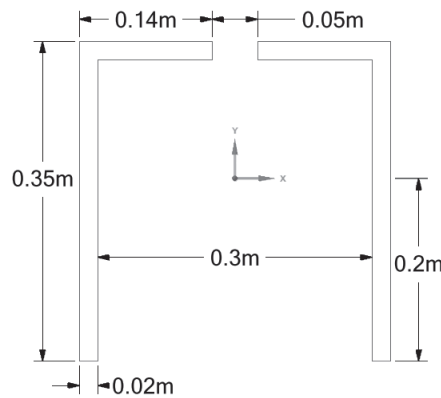

Fig. 2: Two-dimensional design of FOWC used for model 1 with dimensions

The location of 2 wave gauges is shown in Fig. 3, with the dimension specified in Table 5. One wave gauge before, and one inside the chamber of FOWC was deemed to be sufficient for validation purposes. In order to control wave reflection and damping, a numerical beach was added between 7.36m and 9.36m from the FOWC center.
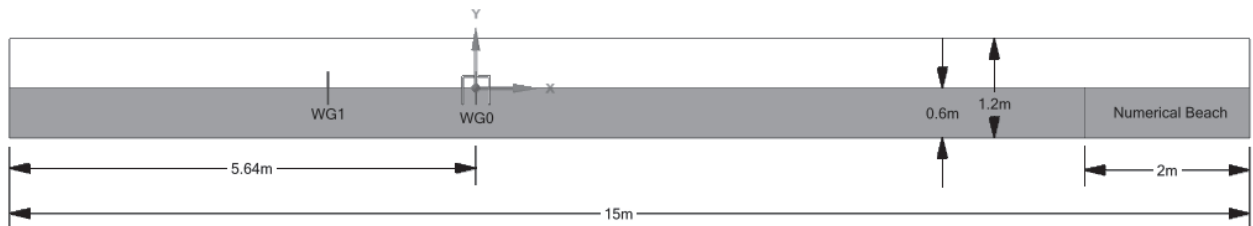

Fig. 3: Schematic of full NWT design for model 1 with the location of wave gauges and numerical beach

Table 5: Label of wave gauge and its distance from the center of FOWC

Wave Gauge	Distance from center of FOWC (m)
WG0	0
WG1	-1.79

For model 2, the design is similar to model with the exception to the differences shown in Fig. 4. Another difference is the flow viscosity, where standard k-epsilon turbulence method is used for all models except model 2, which uses SST

k-omega method. Wave gauge located at the center of FOWC, similar to WG5 in Fig. 6 was used to gather data on wave elevation and velocities in x and y-direction.
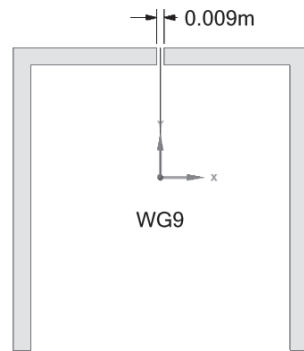

Fig. 4: Two-dimensional design of FOWC used for model 2 with the dimension of the top slot and location of wave gauge

For all models, a fixed mesh setting of 3 different segments was created. As shown in Fig. 5, segment 1 is from the inlet to center, segment 2 is at the center and segment 3 is from center to outlet. For segment 1 and 3, an edge element size of 0.01m with a bias of 10 was set for the height, whereas an edge element size of 0.01m with no bias was set for the length. Face meshing was added for both segments with the cell shape chosen to be quadrilateral. As for segment 2, a face element size of 0.005m with no bias was set.
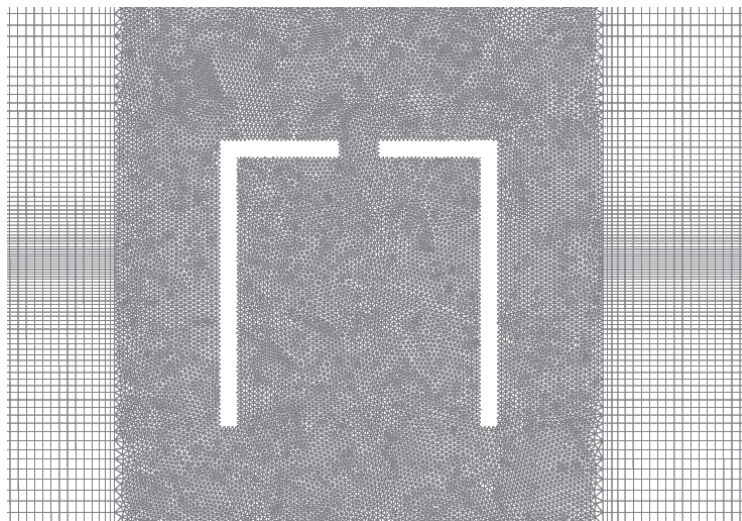

Fig. 5: Schematic of mesh for models 1 and 2. (Segment 1 to the left, segment 2 at center and segment 3 to the right)

2.3 Numerical Set-up for FOWC-breakwater Models

For models 3 to 6, a breakwater is added into the NWT. The design is shown in Fig. 6 and the dimensional specification is shown in Table 6. The gap ratio is calculated based on the gap of FOWC to breakwater, relative to the interior diameter of FOWC. For WG3, WG5, WG6 and WG7, the distance to nearest FOWC or breakwater is maintained to be at 0.01m, this is to ensure that the effect of rigid body on the incident and reflected waves is constant.
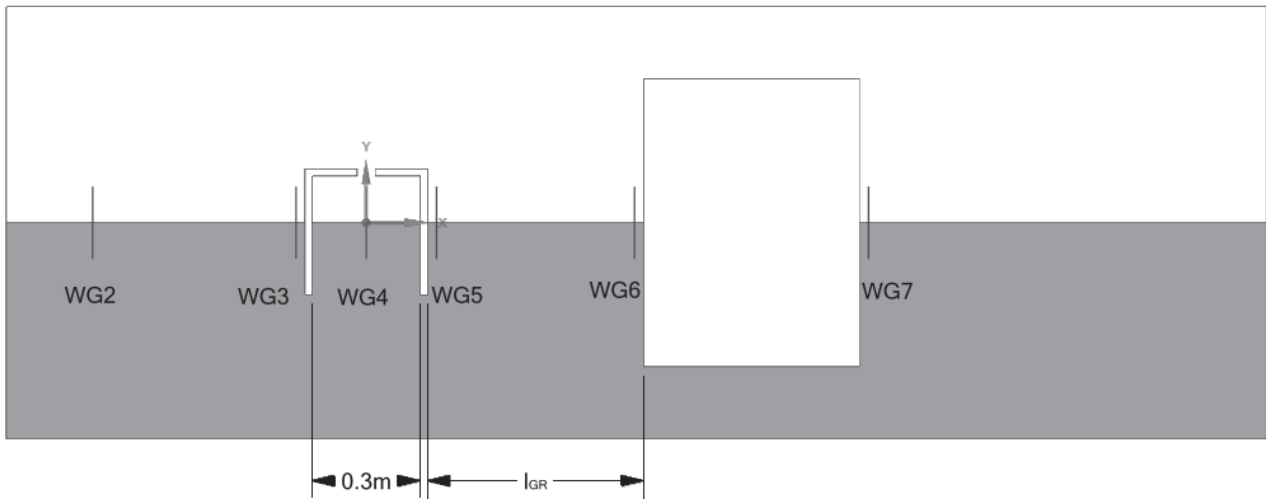
Fig. 6: Schematic of a segment of NWT design for models 3 to 6 with dimensional expressions and location of wave gauges.

Table 6: Gap length and ratio for models 3 to 6

Model	l_{GR}(m)	Gap Ratio
3	0.6	2
4	0.725	2.5
5	0.9	3
6	1.05	3.5

For models 3-6, segment 2 was expanded according to the distance between FOWC and breakwater or increase in the size of breakwater. It was ensured that a gap of 0.13m is available between the edges of segment 2 and FOWC and breakwater, as illustrated in Fig. 7.

Fig. 7: Schematic of mesh for model 3 and 8.

2.4 Governing Equations

ANSYS Fluent solver uses finite volume method (Yamac and Koca, 2019). RANS equations were used. Eq. (1)

– (3) show the mass continuity and Navier–Stokes equations (Fluent, 2013).

$$\frac{\partial(\rho u)}{\partial x} + \frac{\partial(\rho v)}{\partial y} = 0 \tag{1}$$

$$\rho\left(\frac{\partial u}{\partial t} + u\frac{\partial u}{\partial x} + v\frac{\partial u}{\partial y}\right) = -\frac{\partial p}{\partial x} + 2\mu\frac{\partial^2 v}{\partial y^2} + \frac{\partial}{\partial y}\left(\mu\left(\frac{\partial u}{\partial y} + \frac{\partial v}{\partial x}\right)\right) + F_x \tag{2}$$

$$\rho\left(\frac{\partial v}{\partial t} + u\frac{\partial v}{\partial x} + v\frac{\partial v}{\partial y}\right) = -\frac{\partial p}{\partial x} + 2\mu\frac{\partial^2 u}{\partial y^2} + \frac{\partial}{\partial x}\left(\mu\left(\frac{\partial u}{\partial y} + \frac{\partial v}{\partial x}\right)\right) - \rho g + F_y \tag{3}$$

For mass equations, ρ is the fluid density, u is velocity at horizontal direction, v is velocity at vertical direction, x and y are coordinate system directions, μ is the flow viscosity, and F_x and F_y are forces that affect fluid in the vertical and horizontal directions.

The volume fraction of water–liquid at the probe was used to measure wave elevation while the heave motion of FOWC from centroid (average-weighted area) was used to measure the heave movement. The equation used for volume fraction parameter during computation is shown in Eq. (4) (Fluent, 2013).

$$\frac{1}{\rho_q}\left[\frac{\partial}{\partial t}(\rho_q\alpha_q) + \nabla\cdot(\rho_q\alpha_q\,\vec{v}_q)\right] = S_{\alpha_q}\sum_{p=1}^{n}\left(\dot{m}_{pq} - \dot{m}_{qp}\right) \tag{4}$$

Whereby, $\dot{m}_{qp}$ is the instantaneous mass transfer from q-phase to p-phase, $\dot{m}_{pq}$ is the instantaneous mass transfer from p-phase to q-phase, and S_{α_q} is the term of source. Relative error is calculated on the basis of percentage of error of numerical data from present study relative to experimental data (Iturrioz et al., 2015), as shown in Eq. (5) and (6). (Connell and Cashman, 2016)

$$error = \frac{\epsilon_{Numerical} - \epsilon_{Validation}}{\epsilon_{Validation}} \text{ x } 100 \tag{5}$$

Where,

$$\epsilon_{Numerical} = \left(\frac{\epsilon_{max,1} + \epsilon_{max,2} + \epsilon_{max,3} + \epsilon_{max,4} + \epsilon_{max,5}}{5}\right) - \left(\frac{\epsilon_{min,1} + \epsilon_{min,2} + \epsilon_{min,3} + \epsilon_{max,4} + \epsilon_{max,5}}{5}\right) \tag{6}$$

Where $\epsilon_{Numerical}$ is the numerical data for normalized wave elevation and heave movement and $\epsilon_{Validation}$ is the experimental data (Iturrioz et al., 2015) for normalized wave elevation and heave movement. $\epsilon_{max,1}$ to $\epsilon_{min,3}$ refer to the points of the highest and lowest values from the data.

The method used for calculating reflection coefficient is based on Method I from Isaacson (1991), which uses a two fixed probe where two heights and one phase angle is measured. Based on the expression of wave elevation in terms of incident and reflected wave parameters, Eq. (7) was developed, followed by derivations in Eq. (8)-(9):

$$A_i\exp(ikx_n) + A_r\exp[-i(kx_n - \beta)] = A_n\exp[i(\Phi_1 + \delta_n)] \tag{7}$$

$$A_r = \frac{1}{2|\sin\Delta|}\sqrt{A_1^2 + A_2^2 - 2A_1A_2\cos(\Delta + \delta)} \tag{8}$$

$$A_i = \frac{1}{2|\sin\Delta|}\sqrt{A_1^2 + A_2^2 - 2A_1A_2\cos(\Delta - \delta)} \tag{9}$$

Where A_i is the amplitude of incident wave, k is the wave number, x_n is the nth probe location, A_r is the

amplitude of reflected wave, β is the phase angle, A_n is the measured amplitude of the nth record, Φ_1 is the phase angle at first probe, δ_n is the measured phase of the nth wave record relative to the first record. From Eq. (8) and (9), Δ is the dimensionless distance between two probes, A_1 is the measured amplitude of the first record, A_2 is the measured amplitude of the second record. The formula for performance coefficients are shown in Eq. (10)-(16) (He and Huang, 2016) (Zhang et al., 2021).

$$C_r = \frac{A_r}{A_i} \tag{10}$$

$$C_{h,g} = \frac{H_{g,max}}{H_{i,avg}} \tag{11}$$

$$C_{v,g} = \frac{V_{c,avg}}{V_{i,max}} \tag{12}$$

$$C_{h,c} = \frac{H_{c,max}}{H_{i,avg}} \tag{13}$$

$$C_{v,c} = \frac{V_{c,avg}}{V_{i,max}} \tag{14}$$

$$C_{h,t} = \frac{H_{t,max}}{H_{i,avg}} \tag{15}$$

$$C_{v,t} = \frac{V_{t,avg}}{V_{i,max}} \tag{16}$$

Where C_r is the reflection coefficient, $C_{h,g}$ is the wave elevation ratio of the gap region between the FOWC and breakwater versus incident wave, $H_{g,max}$ is the maximum wave elevation in the gap region between the FOWC and breakwater, $H_{i,avg}$ is the average incident wave before the FOWC, $C_{v,g}$ is the velocity ratio of the gap region between the FOWC and breakwater versus incident velocity, $V_{g,avg}$ is the average velocity in the vertical direction in the gap region between the FOWC and breakwater and $V_{i,max}$ is the maximum velocity in the vertical direction of incident wave before FOWC, $C_{h,c}$ is the wave elevation ratio of chamber region versus incident wave, $H_{c,max}$ is the maximum wave elevation inside FOWC chamber, $C_{v,c}$ is the velocity ratio of chamber region versus incident velocity, $V_{c,avg}$ is the average velocity in the vertical direction inside the FOWC chamber, $C_{h,t}$ is the wave elevation ratio of transmission region versus incident wave, $H_{t,max}$ is the maximum wave elevation in the transmission region, $C_{v,t}$ is the velocity ratio of transmission region versus incident velocity, $V_{t,avg}$ is the average velocity in the vertical direction in the transmission region.

3. Results and Discussion

3.1 Results for Validation Models

Result for model 1 shows a relative error from crest to trough of 0.48% at location WG1. Figure 8 shows the result of wave elevation at WG1.
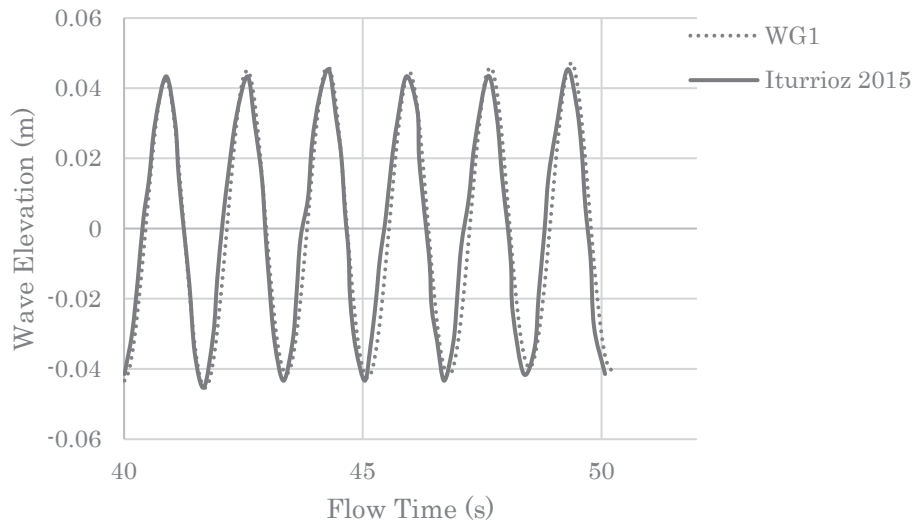
Fig. 8: Graph of wave elevation versus flow time for wave gauge WG1

When model 2 was numerically simulated, the result for horizontal velocity shows a similar range to the result in experimental data, as shown in Fig. 9. The percentage of relative error from crest to trough was not calculated for horizontal velocity because of the inconsistent pattern. From results of both model 1 and 2, it was deduced that the designed numerical models have a reasonable accuracy to experimental data.
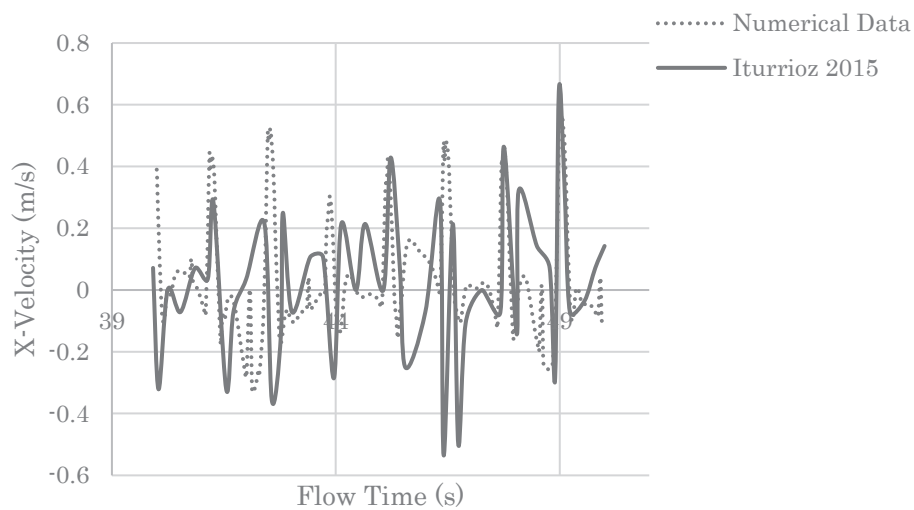

Fig. 9: Graph of horizontal velocity versus flow time

3.2 Results for FOWC-breakwater models

Models 3-6 were used to study the performance of FOWC-breakwater at gap ratios 2, 2.5, 3 and 3.5 and wave periods 1.3s, 1.5s, 1.7s, 1.9s and 2.2s. Firstly, the performance was assessed in terms of C_r, as shown in Fig. 10. Result shows a higher C_r value for gap ratio 3.5, from wave angular frequency of 3-3.5rad/s and 4-4.5rad/s. Ratio 2 shows the lowest C_r value from wave angular frequency range of 3.3-4rad/s, the lowest being 0.07 at 3.3rad/s. Between wave angular frequency range of 3.3-4rad/s, an increasing trend is observed for ratios 2, 2.5 and 3.

Because the reflection coefficient is measured from the incident region, it is favorable to obtain a lower C_r value. This was achieved for all gap ratios at lower wave angular frequencies or higher wave periods from the tested ranges. Gap ratio 2 also shows a lower C_r value on average compared to other gap ratios. This indicates that wave energy transmission to FOWC chamber and beyond is higher at higher wave periods and lower gap ratios from the tested range.

For He and Huang (2016), the x-axis used to plot results is different but comparable to present study; in the latter, wave angular frequency is used but in the former, the ratio of width of WEC versus wavelength was used. The difference in wavelength is proportional to the difference in period in present study. The similarity is that lower or absence of gap could give a lower value of C_r, with an extra advantage being the saving of additional space.

For Zhang et al. (2021), a minimum C_r occurs at wave angular frequency of 3.14rad/s, which is close to the 3.3rad/s for gap ratio 2 in present study. There is also an increase from 3.3-4 rad/s, similar to present study. However, unlike present study, there is no correlation between gap ratio and C_r value. One major point that needs highlighting between present study and Zhang et al. (2021) is the difference in the gap between FOWC and breakwater, which is narrower for all ranges in Zhang et al. (2021) compared to present study.
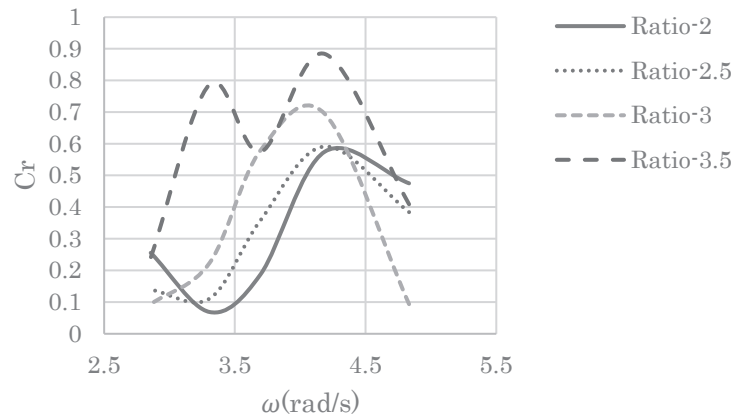

Fig. 10: Graph of reflection coefficient versus angular wave frequency at location WG3 and WG4 for gap ratios 2, 2.5, 3 and 3.5

Results for wave elevation ratio are as shown in Fig. 11. The lowest value recorded was 0.16, which was for $C_{h,t}$ at a wave angular frequency of 4.83rad/s. The highest recorded value was 1.89, which was for $C_{h,g}$ at a wave angular frequency of 2.86 rad/s. There is a similar trend observed in the $C_{h,g}$ and $C_{h,t}$ values, where the trend across the wave angular frequency is decreasing before flattening. This is not observed for $C_{h,c}$, which has a minimum point, before showing an increasing trend.

The noticeably lower values for $C_{h,t}$ compared to $C_{h,g}$ indicates that a significant amount of energy is either extracted or loss in the FOWC chamber and in the gap between FOWC and breakwater. The higher value of $C_{h,c}$ compared to $C_{h,g}$ and $C_{h,t}$ at a higher wave angular frequency indicates that a lower wave period from the tested range is more favorable for higher energy extraction in the FOWC chamber. The opposite is true for $C_{h,g}$, where the most favorable reading was recorded for the highest wave period. As for $C_{h,t}$, a low C_h value is preferred as it indicates that less amount of wave energy is transmitted out of the FOWC-breakwater system. Therefore, the lowest wave period from the tested range showed the most favorable result.

For Zhang et al. (2021) only the wave elevation ratio in the gap region between FOWC and breakwater was measured. The result for all the tested gap ratios showed a maximum value at wave angular frequency ranges of 2.5rad/s to 3.5rad/s before a downward trend was observed. This is similar to the trend shown by $C_{h,g}$ results in present study.
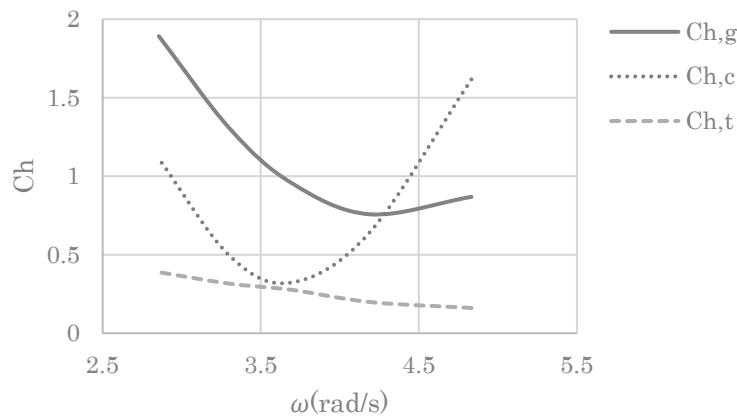
Fig. 11: Graph of wave elevation ratio versus angular wave frequency

Results for velocity ratio, as shown in Fig. 12, show a similar trend as results for wave elevation ratio. The lowest value of 0.07 was recorded for $C_{v,t}$, at a wave angular frequency of 4.83rad/s whereas the highest value of 1.03 was recorded for $C_{v,c}$, at a wave angular frequency of 4.83rad/s.

A major difference between results for wave elevation and velocity ratio is that a higher value was obtained inside the chamber at a lower wave period compared to the gap region between the FOWC and breakwater at a higher wave period, for the wave period ranges tested.

The highest value was also the only value to be above 1, which means that the average vertical velocity in the chamber region was higher than the maximum vertical velocity in the incident region, for wave angular frequency of 4.83rad/s and wave period of 1.3s.
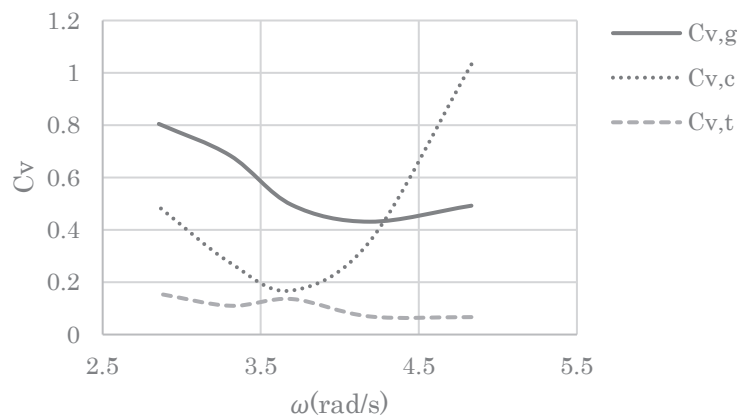
Fig. 12: Graph of velocity ratio versus angular wave frequency

4. Conclusion

A numerical study was conducted on the performance of FOWC-breakwater hybrid system. Firstly models 1 and 2 were used for the purpose of validation with experimental data. Secondly, models of gap ratios 2, 2.5, 3 and 3.5 between FOWC and breakwater were studied for wave periods 1.3s, 1.5s, 1.7s, 1.9s and 2.2s. The performance coefficients that were analyzed are C_r, C_h and C_v.

Results for validation for both models 1 and 2 show a reasonable accuracy with experimental data. For model 1, the a relative error from crest to trough of 0.48% was achieved. For model 2, the result for velocity in the horizontal direction show a similar range to experimental data.

Results for the performance of FOWC-breakwater hybrid system show differences, depending on the regions in the FOWC-breakwater hybrid system.

For the incident region before the FOWC, the C_r values show a more favorable result for lower gap ratio and at a higher wave period. For the FOWC chamber region, the $C_{h,c}$ and $C_{v,c}$ values show a more favorable result for lower wave period. As for the gap region between FOWC and breakwater, $C_{h,g}$ and $C_{v,g}$ values show a more favorable result for higher wave period. For the transmission region after the breakwater, $C_{h,t}$ and $C_{v,t}$ values show a more favorable result for a lower wave period.

All of the results are subject to the range of gap ratios and wave periods tested.

5. Acknowledgements

6. References

Aderinto, T. and Li, H., 2019. Review on power performance and efficiency of wave energy converters. Energies, 12(22), p.4329.

Chen, Z., Yu, H., Hu, M., Meng, G. and Wen, C., 2013. A review of offshore wave energy extraction system. Advances in Mechanical Engineering, 5, p.623020.

Connell, K.O. and Cashman, A., 2016, March. Development of a numerical wave tank with reduced discretization error. In 2016 International Conference on Electrical, Electronics, and Optimization Techniques (ICEEOT) (pp. 3008-3012). IEEE.

De Backer, G., 2009. Hydrodynamic design optimization of wave energy converters consisting of heaving point absorbers. Department of Civil Engineering, Ghent University: Ghent, Belgium.

Fluent, A.N.S.Y.S., 2013. ANSYS fluent theory guide 15.0. ANSYS, Canonsburg, PA, 33.

Goda, Y. and Suzuki, Y., 1977. Estimation of incident and reflected waves in random wave experiments. In Coastal Engineering 1976 (pp. 828-845).

He, F. and Huang, Z., 2016. Using an oscillating water column structure to reduce wave reflection from a vertical wall. Journal of Waterway, Port, Coastal, and Ocean Engineering, 142(2), p.04015021.

Isaacson, M., 1991. Measurement of regular wave reflection. Journal of Waterway, Port, Coastal, and Ocean Engineering, 117(6), pp.553-569.

Iturrioz, A., Guanche, R., Lara, J.L., Vidal, C. and Losada, I.J., 2015. Validation of OpenFOAM® for oscillating water column three-dimensional modeling. Ocean Engineering, 107, pp.222-236.

Kharati-Koopaee, M. and Fathi-Kelestani, A., 2020. Assessment of oscillating water column performance: Influence of wave steepness at various chamber lengths and bottom slopes. Renewable Energy, 147, pp.1595-1608.

Koutrouveli, T.I., Di Lauro, E., das Neves, L., Calheiros-Cabral, T., Rosa-Santos, P. and Taveira-Pinto, F., 2021. Proof of Concept of a Breakwater-Integrated Hybrid Wave Energy Converter Using a Composite Modelling Approach. Journal of Marine Science and Engineering, 9(2), p.226.

LeMéhauté, B., 1969. An introduction to hydrodynamics and water waves (Vol. 52). Environmental Science Servies Administration. Mikami, T., Kinoshita, M., Matsuba, S., Watanabe, S. and Shibayama, T., 2015. Detached breakwaters effects on tsunamis around coastal dykes. Procedia Engineering, 116, pp.422-427.

Samak, M.M., Elgamal, H. and Elmekawy, A.M.N., 2021. The contribution of L-shaped front wall in the improvement of the oscillating water column wave energy converter performance. Energy, 226, p.120421.

Windt, C., Davidson, J. and Ringwood, J.V., 2021. Investigation of Turbulence Modeling for Point-Absorber-Type Wave Energy Converters. Energies, 14(1), p.26. Yamac, H.I. and Koca, A., 2019. Shore type effect on onshore wave energy converter performance. Ocean Engineering, 190, p.106494.

Zhang, H., Zhou, B., Vogel, C., Willden, R., Zang, J. and Geng, J., 2020. Hydrodynamic performance of a dual-floater hybrid system combining a floating breakwater and an oscillating-buoy type wave energy converter. Applied Energy, 259, p.114212.

Zhang, H., Zhou, B., Zang, J., Vogel, C., Fan, T. and Chen, C., 2021. Effects of narrow gap wave resonance on a dual-floater WEC-breakwater hybrid system. Ocean Engineering, 225, p.108762.

Zhao, X.L., Ning, D.Z., Zou, Q.P., Qiao, D.S. and Cai, S.Q., 2019. Hybrid floating breakwater-WEC system: A review. Ocean engineering, 186, p.106126.